Performance Evaluation of Threshold -Based TOA Estimation Techniques Using IR-UWB Indoor Measurements

Lei Yu, Mohamed Laaraiedh, Stéphane Avrillon, Bernard Uguen, Julien Keignart, Julien Stéphan

Performance Evaluation of Threshold-Based TOA Estimation Techniques Using IR-UWB Indoor Measurements

Lei Yu⋆, Mohamed Laaraiedh⋆, Stéphane Avrillon⋆, Bernard Uguen⋆, Julien Keignart‡, Julien Stephan♯
⋆ Université de Rennes 1, IETR, Campus Beaulieu Bat 11D, Rennes 35042 France
‡ CEA Leti Minatec, 17 Rue des Martyrs 38054 Grenoble, France
♯ SIRADEL, 3 Allée Adolphe Bobierre CS 24343, 35043 RENNES France
Email : [lei.yu, mohamed.laaraiedh, stephane.avrillon, bernard.uguen]@univ-rennes1.fr, julien.keignart@cea.fr, jstephan@siradel.com

***Abstract*— Ultra-wide bandwidth (UWB) technology is a viable candidate for enabling accurate localization through time of arrival (TOA) based ranging techniques. These ranging techniques exploit the high time resolution of the UWB signals to estimate the TOA of the first signal path. Nevertheless, these techniques are facing the problem of proper multipath mitigation especially in harsh propagation environments in which the first path may not exist or it may not be the strongest. This paper presents a realistic comparison between the ranging performances of four threshold-based TOA estimation techniques using experimental data collected from an IR-UWB indoor propagation measurement campaign performed in an office building.**

***Index Terms*— TOA, Ranging techniques, Channel impulse response, IR-UWB, Measurements, Indoor positioning**

I. Introduction

Ultra wide-band (UWB) is a viable technology for short-range wireless indoor communication with a number of attractive features: high-rate transmission, low complexity, low cost, and low-power consumption [1], [2]. This technology has generated considerable and increasing interest by many manufacturers since February 2002, when the Federal Communication Commission (FCC) opened up 7.5 GHz of spectrum (from 3.1 GHz to 10.6 GHz) for use by UWB devices. The traditional design approach for an UWB communication system uses narrow time-domain pulses of very short duration, typically on the order of a nanosecond, thereby spreading the energy of the radio signal quite uniformly over a wide frequency band ranging from extremely low frequencies to a few gigahertz [3], [4]. This method is usually called impulse radio UWB (IR-UWB). A great advantage of the short pulse modulation is the possibility to estimate the TOA with a fine resolution, which translates in ranging estimation with a less than one meter accuracy allowing for many location and tracking applications. The two main ranging techniques defined for IR-UWB are One Way Ranging (OWR) and Two Way Ranging (TWR) [4], [5], [6].

Using channel (impulse) responses -C(I)R-, different techniques have been proposed for estimating TOA. The simplest and easiest technique estimates the TOA as the time of arrival of this strongest path [6], [7]. However, this assumption is not usually true in multipath conditions. In such conditions, we distinguish two cases: the Line-of-Sight (LOS) in which no obstacle separates the Tx and the Rx and the Non-Line-of-Sight (NLOS) if the obstacle exists. In the LOS case, the strongest path is usually the first path while in the NLOS case the first path may be more attenuated than indirect paths [8]. Hence, we need more advanced techniques to extract this first path and estimate the TOA. The reader can refer to [3], [9] and references therein for more details about the techniques already proposed for TOA ranging within IR-UWB signals.

In that direction, this paper presents a contribution to the TOA estimation techniques based on IR-UWB channel responses. Four techniques are presented and studied using an IR-UWB measurements campaign. The first technique is typical and widely used. It is based on the setting of a threshold above the noise floor to detect the first ray. Based on this first technique, we derivate three different techniques. The second technique is a modified version of the first one and uses the cumulative CR instead of the CR. The third technique is based on the detection of the first strongest paths using a dichotomous search approach. The fourth and last technique is a combination of the first and third techniques.

The rest of the paper is organized as follows. We start in section II by giving the assumed channel model. Then, we details in section III the different techniques of TOA estimation. In section IV, the UWB measurement campaign is presented. This measurement campaign is used to tune, evaluate, and compare the different presented techniques. Finally, the results are discussed in section V and our concluding remarks are given in section VI.

II. UWB Channel impulse response model

For all the rest of the paper, we consider a multipath channel with a CIR modeled as the sum of all received pulses as follows:

$$c(t) = \sum_{n=1}^{N} a_n \delta(t - \tau_n) \tag{1}$$

where a_n and τ_n are, respectively, the amplitude and time-delay of the nth propagation path; τ_1 is the time of arrival of

the first path (i.e. The TOA between the Tx and the Rx) which we seek to find out.

The received signal can then be expressed as:

$$r(t) = \sum_{n=1}^{N} a_n \omega(t - \tau_n) + n(t) = s(t - \tau_1) + n(t) \quad (2)$$

where $\omega(t)$ is the isolated ideal received pulse with duration T_p (i.e. in the absence of multipath and noise) and $n(t)$ is the additive white Gaussian noise (AWGN) with zero mean and spectral density $N_0/2$ where N_0 is the noise power density. $s(t)$ is the noise-free CIR defined as:

$$s(t - \tau_1) = \sum_{n=1}^{N} a_n \omega(t - \tau_n) \quad (3)$$

In all the rest of this paper, we use the sampled form of $r(t)$ with a sample rate $1/T_s$ where T_s is the sample duration. Let M be the number of samples which compose $r(t)$. Hence, if the received signal is observed in the interval $[0, T]$, we get $T = MT_s$. The mth sample occurs at the time $t_m = mT_s$ ($m \in (1, ..., M)$).

Given a channel response modeled by (2), the goal is to estimate τ_1, i.e. the TOA of the first path. In the next section, four different techniques for estimating TOA will be described.

III. Techniques of TOA estimation based on UWB signals

This section presents the different techniques for estimating TOA from the UWB signals. These techniques are numerated from 1 to 4 as follows:

- *T1*: Setting a threshold above the noise floor
- *T2*: Setting a threshold above the cumulative noise floor
- *T3*: Dichotomous left interval selection
- *T4*: Thresholded dichotomous left interval selection

A. T1: *Setting a threshold above the noise floor*

This approach is the most typical and has been proposed by *Lee* and *Scholtz* in [10]. This technique starts by defining a threshold γ_{th} which must be above the noise level in order to limit as much as possible false alarm on noise peak while maintaining a sufficient level of detection. The implementation of this technique involves the following steps:

- Consider the squared channel response $r^2(t)$;
- Compare the actual value of $r^2(t)$ to the appropriate threshold γ_{th};
- Search the first crossing point and let m be the corresponding sample. The TOA estimate $\hat{\tau}_1^{th}$ is then given by mT_s.

The choice of the threshold is the most challenging task in such technique. As shown in Fig. 1, which plots an example of measured CR, the probability of detecting noise peaks (false alarm) is higher with an underestimated threshold. Whereas, with an overestimated threshold, it is the probability of skipping the direct path which is higher. In [11], different methods for choosing the threshold are described and compared. In this paper, we have chosen to statistically define the threshold relatively to the maximum value of the signal using the available UWB measurements (see section V below).

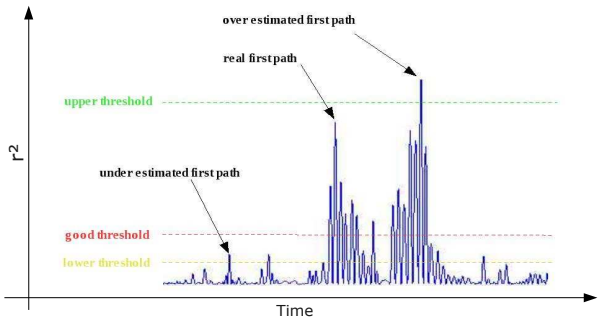

Fig. 1. *T1* -Setting a threshold above the noise floor- : the threshold must be fairly chosen in order to avoid under- and over- estimation of the TOA.

B. T2: *Setting a threshold above the cumulative noise floor*

In this technique, we propose to apply a threshold on the cumulative received signal instead of the simple received signal in technique *T1*. For this, the ecdf (energy cumulative density function) $c_r(t)$ of the received signal $r(t)$ is defined and it is given, at time τ by:

$$\begin{aligned} c_r(\tau) &= \int_0^\tau r^2(t)\,dt \\ &= \int_{\tau_1}^\tau s^2(t-\tau_1)dt + \int_0^\tau n^2(t)dt \\ &\quad +2\int_{\tau_1}^\tau s(t-\tau_1)n(t)dt \end{aligned} \quad (4)$$

where $s(t)$ is defined in (3). Then, we obtain:

$$c_r(\tau) = E_s([\tau_1, \tau]) + c_n(\tau) + 2\int_{\tau_1}^{\tau} s(t-\tau_1)n(t)dt \quad (5)$$

where $E_s([\tau_1, \tau])$ represents the integrated energy of the useful signal between τ_1 and τ and $c_n(\tau)$ represents the integrated noise between 0 and τ. The last integral ($\int_{\tau_1}^{\tau} s(t-\tau_1)n(t)dt$) can be neglected assuming independence between signal and noise. This leads to the following expression:

$$c_r(\tau) \approx E_s([\tau_1, \tau]) + c_n(\tau) \quad (6)$$

After the construction of this cumulative signal, the same steps presented for technique *T1* are applied (see Fig. 2). That is to say:

- Compute the cumulative received signal c_r;
- Compare the actual value of c_r to the appropriate threshold γ_{cum};
- Search the first crossing point and let m be the corresponding sample. The TOA estimate $\hat{\tau}_1^{cum}$ is then given by mT_s.

C. T3: *Dichotomous left interval selection*

This technique seeks to estimate properly TOA values associated with situations where the strongest path is not the first path (but it is still valid in LOS situations). This technique

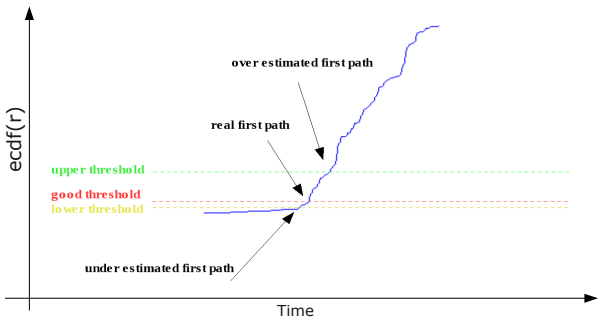

Fig. 2. *T2* -Setting a threshold above the cumulative noise floor-: the threshold is now applied on the cumulative channel response. The figure plots an example of an ecdf obtained from measurements.

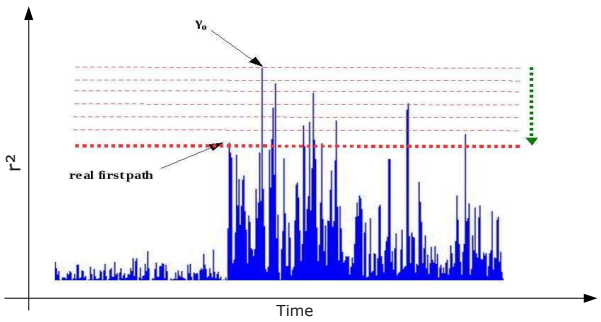

Fig. 3. *T3* -Dichotomous left interval selection-: the technique estimates the TOA as the time of arrival of the first path among N_{max} strongest paths determined using a dichotomous algorithm.

proposes to consider the largest N_{max} peaks of the received signal. A receiver can easily search these strongest paths. The TOA is then estimated as the time delay of the peak with the smallest index (see Fig. 3). In this technique, the key parameter is N_{max} which is the number of the largest signal peaks. In this work, N_{max} is chosen statistically using the UWB measurement campaign. The pseudo-code of this technique is given by Algorithm 1.

Algorithm 1 Dichotomous left interval selection

$\gamma_0 \leftarrow \max\{r^2(\tau)\}$: compute the peak energy
set N_{max}: the key parameter
$\gamma \leftarrow \gamma_0$: initialize the threshold
$N_{int} \leftarrow 1$: initialize the number of current intervals
$\epsilon \leftarrow 10^{-2}$: set the the decreasing factor
while $N_{int} < N_{max}$ **do**
  $\mathbf{T}_\gamma \leftarrow$ *GetIntervals*$(r^2(\tau), \gamma)$: compute the valid time support
  $N_{int} \leftarrow$ *NumberofIntervals*$(\mathbf{T}_\gamma)$: update the number of intervals (strongest peaks)
  $\gamma \leftarrow \gamma(1-\epsilon)$: decrease the threshold by ϵ
end while
$\hat{\tau}_1^{max} \leftarrow \min\{\mathbf{T}_\gamma\}$: estimate the TOA

$\mathbf{T}_\gamma$ is a union of intervals which corresponds to the delay values where the squared received signal is above a threshold γ. This set of intervals is determined via a dichotomous algorithm which stops when the preassigned value of interval N_{max} has been reached. The estimated delay is then chosen as the minimum value of this interval. This pseudo-code defines two elementary function *GetIntervals* and *NumberofIntervals* which respectively return the time support where $r^2(\tau) > \gamma$ and the number of disjoint intervals from a union of intervals given as an input. This approach is different in nature from both jump back and search forward (JBSF) and seek backward scheme (SBS) described in [3] and [12]. There is no threshold to be defined from a-priori knowledge of the channel parameters.

D. T4: *Thresholded dichotomous left interval selection*

This technique mixes the threshold-based technique (*T1*) and the left interval technique (*T3*) in a search-back window in order to detect the first arrival path (see Fig. 4). The estimator involves the following steps:

1) Find the strongest path and calculate the peak energy γ_0;
2) Find the peak energy γ_{noise} in the noise part of the CR by defining a common time slot (0-5ns in our case);
3) Set a fixed size search-back window, from 0 to the strongest path, in order to estimate the TOA;
4) Decrease the threshold γ gradually from the peak energy γ_0 and calculate the number of intervals in the defined search-back window;
5) Calculate the ratio $\gamma - \gamma_{noise}/\gamma_0\epsilon$ and stop the algorithm when the ratio is relatively close to α which is the key parameter defined to best fit the measurements;
6) Search the first crossing point and let m be the corresponding sample. The TOA estimate $\hat{\tau}_1^{win}$ is then given by mT_s.

The pseudo code of this technique is given by Algorithm 2.

Algorithm 2 Thresholded dichotomous left interval selection

set α: the key parameter
$\gamma_{noise} \leftarrow \max\{r^2(\tau)\}$ $\tau \in [0, 5ns]$
$\gamma_0 \leftarrow \max\{r^2(\tau)\}$
compute τ_0: TOA of the strongest path
$win \leftarrow [0, \tau_0]$: define the search-back window
$\gamma \leftarrow \gamma_0$
$\epsilon \leftarrow 10^{-2}$: decreasing factor
while $\frac{\gamma - \gamma_{noise}}{\gamma_0 \epsilon} > \alpha$ **do**
  $\mathbf{T}_{\gamma,\mathbf{win}} \leftarrow \texttt{GetIntervals}(r^2(\tau), \gamma, win)$
  $\gamma \leftarrow \gamma(1-\epsilon)$: decrease the threshold by ϵ
end while
$\hat{\tau}_1^{win} \leftarrow \min\{\mathbf{T}_{\gamma,win}\}$

IV. UWB Measurement Campaign

The measurements campaign has been carried out, within the framework of the *FP7-WHERE* project, by *CEA-LETI*

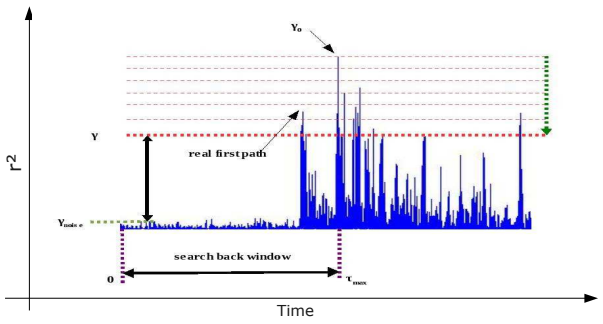

Fig. 4. *T4* -Thresholded dichotomous left interval selection-: the technique searches the strongest paths in a predefined window going from zero to the strongest path.

in the *SIRADEL* headquarter building in Rennes, France. The goal was to collect UWB channel responses in a same local area. In order to assess small-scale fading, channel response measurements are made on several square grids. This measurements campaign is dedicated for the evaluation and validation of localization techniques and algorithms.

The time-domain channel sounder is mainly composed of a pulse pattern generator, a wide band digital oscilloscope, and UWB antennas. The whole measurement setup is illustrated in Fig. 5 [13]. On the transmitter side, a Pulse Generator (Picosecond Pulse Lab 4050B) with two additional impulse forming networks and a power amplifier fit the desired UWB impulse shape in the $3-7$ GHz bandwidth (see Fig. 6). On the receiver side, a wide-band Digital Oscilloscope (*Tektronix TDS 6124C*) is used with a sampling rate of 20 Gsps in real-time. In order to improve the time precision, a *sinc* interpolation is used in order to get a final time step of 5ps. Moreover, the signal is averaged over 16 snapshots for increasing the signal-to-noise ratio (SNR). For dynamic range consideration, it is also necessary to use Low Noise Amplifiers in front of oscilloscope input channels. On both Tx and Rx sides the same kind of antenna is used. The radiation pattern is omni-directional in azimuth with a bipolar radiation pattern in elevation [14].

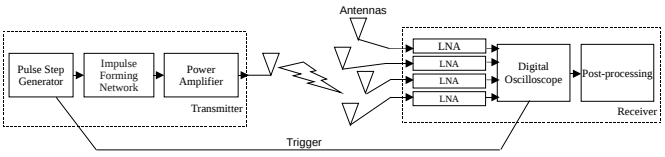

Fig. 5. Overall measurement chain used to perform UWB measurements.

During the campaign, four fixed receiver positions were defined and 302 measurement points were selected for the transmitter positions [14] with the transmitter and the four receivers at the same height (120cm between the floor and the antenna ground plan). Fig. 7 shows the different positions of transmitters and receivers. The most important pieces of furniture (metallic cupboards and tables) should be taken into consideration when modeling the channel propagation and estimating TOA in order to better understand the effects of

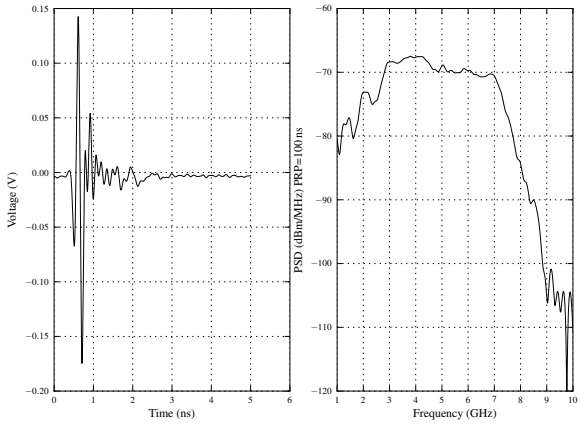

Fig. 6. UWB impulse feeding the Tx antennas.

radio propagation, channel characteristics, and environment components on extracted TOA. These furniture pieces are presented in Fig. 8. Nevertheless, many other small pieces of furniture (chairs, printers, refrigerator, etc) are present when performing measurements. Taken into consideration all these small furnitures in channel modeling is a hazardous task. Hence, the choice was been made not to consider these small furnitures.

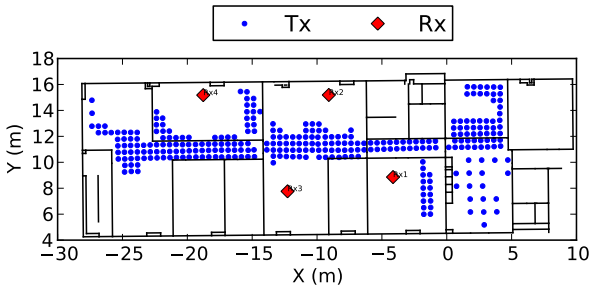

Fig. 7. Rx and Tx locations defined in the *SIRADEL* environment.

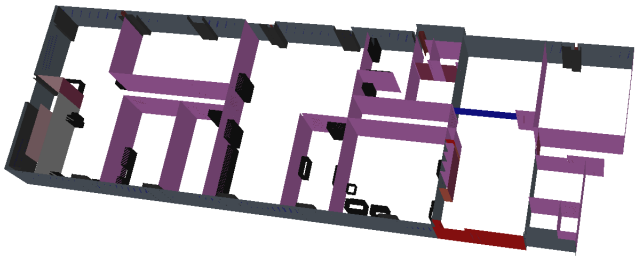

Fig. 8. Top view of investigated rooms in the first floor of Siradel building.

When performing channel sounding, it is necessary to extract exclusively the channel behavior (with or without antennas) by using appropriate calibration procedures based on deconvolution tools [15]. These calibration procedures aim to eliminate the effects of all the elements involved in the

link like PA, cable, and LNAs. For each Tx-Rx pair, we store the CR measured by the sounder. In addition to the CR, different parameters are saved in each profile mainly Tx and Rx positions accurately measured, date, and time [14]. We define also the link quality indicator (LQI) as the ratio between the maximum signal amplitude and the maximum noise amplitude estimated during the first five nanoseconds corresponding to a common time slot without any signal [14]. The LQI gives an indication about the SNR of the received signal. The ranging techniques will hence be evaluated for different values of the LQI (i.e. the SNR).

V. Results and Discussions

The four presented techniques in section III are dependent on key-parameters which have to be adequately chosen in order for the technique to perform higher ranging accuracy. The determination of optimal key-parameters is not the object of this paper. In order to make a fair comparison between the four techniques, we set the key-parameters to the values which fit the best the available measurements. Nevertheless, these key parameters can be fixed in a more optimal way in order to guarantee more enhanced performances. These parameters can be chosen for example with respect to the SNR values or based on received signal statistics [3].

A. Tuning of different techniques using the measurement campaign

The figures (a) to (d) in Fig. 9 represent the average absolute ranging error as a function of key parameter values respectively for the four techniques. In each figure, the key-parameter which gives the best average ranging accuracy is chosen. These figures give a parametric evaluation of the different techniques and highlight the importance of choosing the best value for the key parameter in order to reach the highest ranging accuracy.

In the rest of this paper, the chosen key-parameters are:

- Technique *T1*: γ_{th}/γ_0 = 0.14
- Technique *T2*: γ_{cum} = 0.04
- Technique *T3*: N_{max} = 16
- Technique *T4*: α = 13

B. Comparison of different techniques

In order to compare the four TOA ranging techniques, we consider the UWB measurement campaign described before and we apply the different techniques on the 302 Tx positions. In total, we got $302 \times 4 = 1208$ TOA estimates. First, we plot in Fig. 10 the evolution of the average ranging error with respect to the LQI values. This figure reveals that at higher SNR, the four techniques achieve close ranging accuracy which tends to 3cm. For lower SNR, the *T4* technique achieves the best performances while the typical *T1* technique is not reliable at all. The techniques *T2* and *T3* outperform the *T1* technique at lower and medium SNR. These results outperform the results proposed in [16] and approaches those presented in [12] where no real measurement campaign was used to evaluate the performances of ranging techniques. Indeed, these

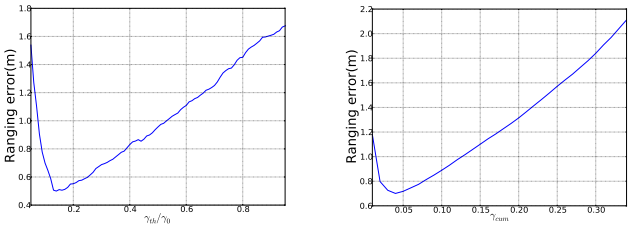

(a) Evolution of statistical repartition of error on estimated ToA as a function of γ_{th}/γ_0

(b) Evolution of statistical repartition of error on estimated toa as a function of γ_{cum}

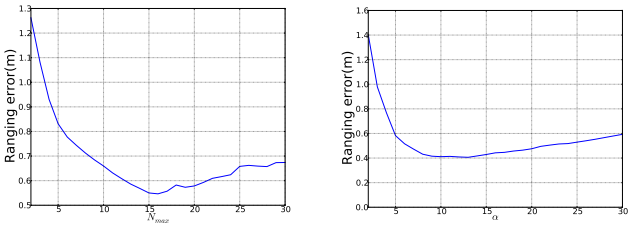

(c) Evolution of statistical repartition of error on estimated toa as a function of N_{max}

(d) Evolution of statistical repartition of error on estimated toa as a function of α

Fig. 9. Tuning of different ranging techniques using UWB measurements: the key-parameters are chosen to best fitting the measurements.

two papers used simulation models (CM1, ..., CM4), which are more or less simplified and do not accurately represent the reality of the radio channel. In our work, the goal was to evaluate the ranging techniques on a real measurements campaign in order to outcome the limits of such techniques. In the rest of this section, we will present the performances for links with a LQI higher than 10dB.

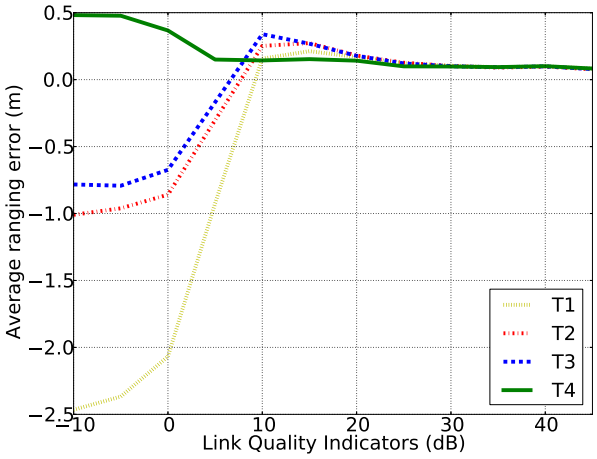

Fig. 10. Average Ranging error wrt. LQI for different techniques.

The overall comparison is given in Fig. 11 and Table I while the comparison between these techniques in LOS, NLOS, and NLOS^2 cases are given respectively in Table II. The LOS case is a situation where no obstacle is located between the Tx and

the Rx. If an obstacle exists, we have no visibility between the Tx and the Rx and we differ two cases: the NLOS case where a direct path crosses the obstacle and reach the Rx and the NLOS^2 case where no direct path is crossing the obstacle. In each figure, we plot the cumulative density function (cdf) of the ranging error for the four different techniques. Fig. 11 shows that the *T4* technique outperforms the three other techniques. Table I shows that the lower mean ranging error and standard deviation are performed by the fourth technique (*T4*) which is based on the fusion of *T1* and *T3* techniques. It benefits thus from the advantages of these two techniques to give the best ranging accuracy. With a real measurement campaign, we believe that the obtained accuracy of 13cm as a mean value and 50cm as a deviation value is very promising compared to results presented in [6], [12], [16], [17]. Notice also that the choice of the key parameter of each technique should be done in a more optimal way in order to enhance the ranging accuracy.

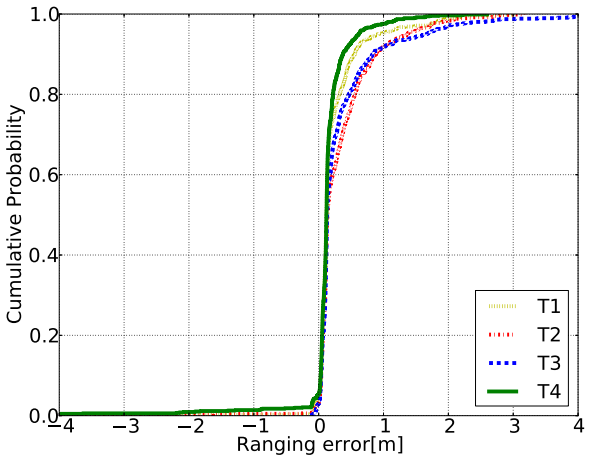

Fig. 11. CDF of ranging error performed by the four techniques for an LQI $\geq$ 10dB.

TABLE I

STATISTICAL TOA BASED RANGING MODELS EXTRACTED FROM UWB INDOOR MEASUREMENTS CAMPAIGN FOR LQI$>$ 10DB.

Technique	Mean(m)	STD(m)
T1	0.22	0.44
T2	0.33	0.55
T3	0.36	0.64
T4	0.13	0.50

Table II presents the ranging accuracy for different visibility conditions. The table reveals that the four techniques give the same performances in LOS conditions. This is obvious because the direct path (the strongest one) is easily distinguished in LOS conditions. In these conditions the ranging precision is up to 8cm. However, in the NLOS and NLOS^2 conditions which are the most common situations inside a building with furnitures, we can see different performances for different techniques.

TABLE II

STATISTICAL TOA BASED RANGING MODELS EXTRACTED FROM UWB INDOOR MEASUREMENTS CAMPAIGN FOR LQI$>$ 10DB FOR DIFFERENT VISIBILITY CONDITIONS.

Visibility	Technique	Mean(m)	STD(m)
LOS	*T1*	0.08	0.03
	T2	0.07	0.03
	T3	0.08	0.36
	T4	0.08	0.36
NOS	*T1*	0.16	0.26
	T2	0.22	0.32
	T3	0.20	0.34
	T4	0.11	0.22
NLOS^2	*T1*	0.31	0.56
	T2	0.48	0.68
	T3	0.54	0.80
	T4	0.16	0.66

In some NLOS and NLOS^2 situations, it occurs that the signal is obstructed by a metallic cabinet which makes the detection of the first ray very difficult and the ranging accuracy very poor. This is shown in Fig. 12 where we plot the distribution of ranging error for the four receivers using the *T4* technique. In this figure, the positions obstructed by metallic cabinets show a low ranging accuracy. These metallic cabinets deeply affect the TOA ranging accuracy. In order to better model and exploit TOA within localization applications under the presence of such obstructing objects, TOA models should be spatially particularized as shown in [18].

VI. CONCLUSION

This paper presented a study of four different ranging techniques applied to IR-UWB technology. Using an IR-UWB measurements campaign, these four techniques are tuned, evaluated, and compared. The paper presented the typical threshold-based TOA estimation technique and proposed a modified version using the cumulative channel impulse response. We proposed also a dichotomous based technique which outperforms the cumulative CIR based technique. The fourth and last technique is a fusion of the two techniques: threshold based and dichotomous based. This technique benefits from the advantages of these two techniques and outperforms hence all the studied techniques. The main outcome of this paper was to study the performances of ranging techniques on a real UWB measurement campaign unlike the most of existing works which are based on simplified simulation models. The paper shows that the reached accuracy with this real measurements campaign is very promising compared to the state of the art.

ACKNOWLEDGMENT

This work has been performed in the framework of the ICT project ICT-248894 WHERE2, which is partly funded by the European Union.

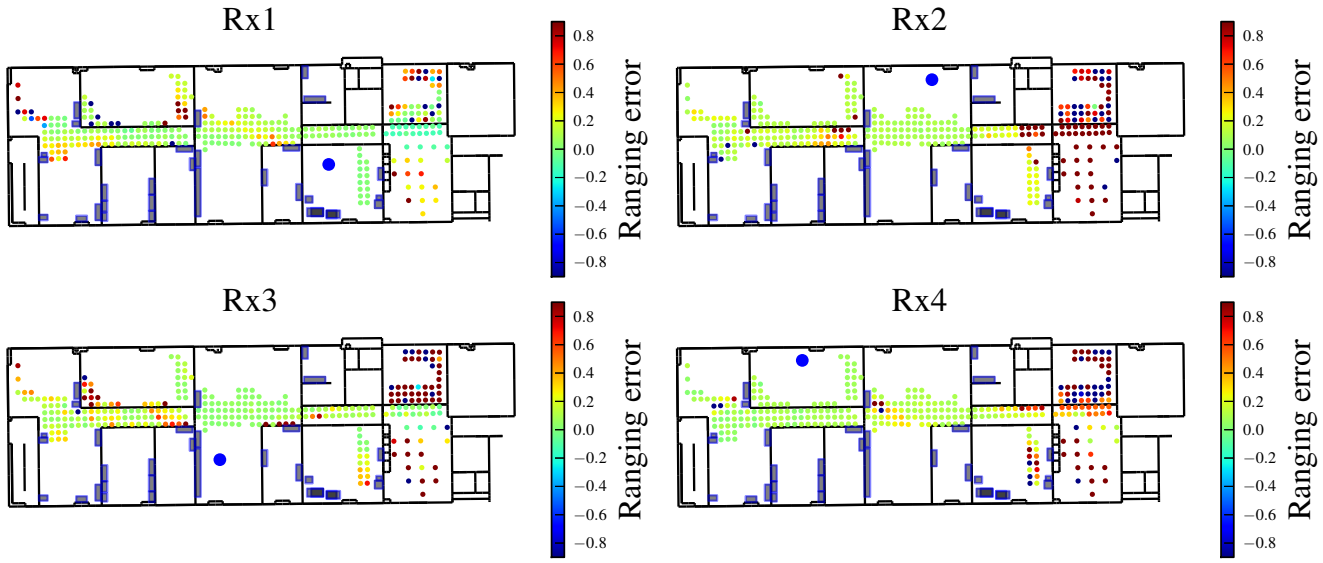

Fig. 12. Mapping of ranging error obtained with the *T4* technique for the different receivers. The figure highlights the effect of metallic cupboards on the ranging accuracy.

REFERENCES

[1] M. Z. Win and R. A. Scholtz. Impluse radio: How it works. *IEEE Communications Letters*, 2(2):36–38, February 1998.

[2] A. F. Molisch, P. Orlik, Z. Sahinoglu, and J. Zhang. UWB-based sensor networks and the IEEE 802.15.4a standard - a tutorial. *Proceedings of the IEEE First International Conference on Communications and Networking ChinaCom'06*, pages 1–6, October 2006.

[3] I. Guvenc, S. Gezici, and Z. Sahinoglu. Ultra-wideband range estimation: Theoretical limits and practical algorithms. In *Ultra-Wideband, 2008. ICUWB 2008. IEEE International Conference on*, volume 3, pages 93–96, sept. 2008.

[4] S. Gezici, Z. Tian, G. B. Giannakis, H. Kobayashi, A. F. Molisch, H. V. Poor, and Z. Sahinoglu. Localization via ultra-wideband radios: a look at positioning aspects for future sensor networks. *IEEE Signal Processing Magazine*, 22(4):70–84, 2005.

[5] B. Denis, L. Ouvry, B. Uguen, and F. Tchoffo-Talom. Advanced bayesian filtering techniques for uwb tracking systems in indoor environments. page 6 pp., September 2005.

[6] D. Dardari, A. Conti, U. Ferner, A. Giorgetti, and M. Z. Win. Ranging with ultrawide bandwidth signals in multipath environments. *Proceedings of the IEEE*, 97(2):404–426, February 2009.

[7] G. Bellusci, G. J. M. Janssen, J. Yan, and C. C.J.M. Tiberius. A new approach to low complexity uwb indoor los range estimation. pages 1–6, September 2008.

[8] F. Li, W. Xie, J. Wang, and S. Liu. A new two-step ranging algorithm in nlos environment for uwb systems. In *Communications, 2006. APCC '06. Asia-Pacific Conference on*, pages 1–5, August 2006.

[9] D. Dardari, C. Chong, and M.Z. Win. Threshold-based time-of-arrival estimators in uwb dense multipath channels. *IEEE Transactions on Communications*, 56(8):1366–1378, August 2008.

[10] J. Lee and R.A. Scholtz. Ranging in a dense multipath environment using an UWB radio link. *IEEE Journal on Selected Areas in Communications*, 20(9):1677–1683, December 2002.

[11] I. Guvenc and Z. Sahinoglu. Threshold-based TOA estimation for impulse radio UWB systems. *Proceedings of IEEE International Conference on Ultra-Wideband (ICU05)*, pages 420–425, September 2005.

[12] C. Falsi, D. Dardari, L. Mucchi, and M. Z. Win. Time of arrival estimation for uwb localizers in realistic environments. *EURASIP Journal on Applied Signal Processing*, 2006:152–152, January 2006. ISSN 1110-8657.

[13] J. Keignart, C. Abou Rjeily, N. Daniele, and C. Delaveaud. UWB SIMO channel measurements and simulations. *IEEE Transactions on Microwave Theory and Techniques, Special Issue on Ultra-Wideband*, 54(4):1812–1819, April 2006.

[14] ICT-217033-WHERE-Project. Deliverable 4.1: Measurements of location-dependent channel features, October 2008.

[15] B. Denis and J. Keignart. Post-processing framework for enhanced UWB channel modeling from band-limited measurements. *Proceedings of IEEE UWBST Conference, Reston, VA*, pages 260–264, November 2003.

[16] A. Hernandez, R. Badorrey, J. Choliz, I. Alastruey, and A. Valdovinos. Accurate indoor wireless location with ir uwb systems a performance evaluation of joint receiver structures and toa based mechanism. *IEEE Transactions on Consumer Electronics*, 54(2):381–389, May 2008.

[17] D. Dardari, A. Giorgetti, and M.Z. Win. Time-of-arrival estimation of uwb signals in the presence of narrowband and wideband interference. In *Ultra-Wideband, 2007. ICUWB 2007. IEEE International Conference on*, pages 71–76, September 2007.

[18] B. Uguen, M. Laaraiedh, B. Denis, J. Keignart, J. Stephan, and Y. Lostanlen. Extraction and characterization of location-dependent uwb radio features with practical implications for indoor positioning. In *In proceedings of IEEE EW conference, EW2012*, April 2012.